PAPER S

ANALYSIS OF NOISES AFTER PRESTACK MIGRATION IN CROSSWELL SEISMIC PROFILING

Le-Wei Mo

ABSTRACT

Pre-stack Kirchhoff migration equations for cross-well seismic survey in medium with arbitrary velocity variations are derived. Migration operation increases signal/noise ratio. We show that S/N ratio is much higher in migration images than in common shot gather data.

Radiation angle transformation helps separating signal from noise in pre-stack migration images. We show that channel wave events in common angle images dip at the radiation angle. Transmission multiple reflection events in common angle images appear vertical. Slant stack dip filtering is used to attenuate these two kinds of noises.

KIRCHOFF MIGRATION

In this section, I derive the Kirchhoff migration integral for a medium with arbitrary velocity variations, for prestack migration of single source and multiple receiver multi-channel data. The application is for prestack migration of cross-well seismic data, in particular. Begin with the Helmholtz equation,

$$(\nabla^2 + \omega^2 / v^2)G = \delta(r - r_1) \qquad (1)$$

G is the function which solves equation (1) and satisfies the radiation conditions (Goodman, 1970); ∇^2 is the Laplacian operator, ω is frequency, $v(x,z)$ is acoustic velocity, and δ is the Dirac delta function. Later, r and r_1 will turn out to be the position vectors of the source/receiver pair and point scatterer, respectively. The wave field $P(r,\omega)$ satisfies the equation

$$(\nabla^2 + \omega^2 / v^2)P(r,\omega) = 0 \qquad (2)$$

inside the source-free volume V. To obtain the Kirchhoff integral, we use the Green's second theorem,

$$\int_V (\phi_1 \nabla^2 \phi_2 - \phi_2 \nabla^2 \phi_1) dV = \int_S (\phi_1 \partial_n \phi_2 - \phi_2 \partial_n \phi_1) dS \qquad (3)$$

where n denotes the outward normal direction to the surface S, and substitute $\phi_1 = P(r,\omega)$, and $\phi_2 = G$ to obtain

$$P(r_1,\omega) = \int_S (P(r,\omega)\partial_n G - G\partial_n P(r,\omega)) dS \qquad (4)$$

which is the Kirchhoff integral.

In the Kirchhoff integral equation (4), both the wave field records $P(r,\omega)$ and its gradient are required. But in actual seismic profiling, only the wave fields $P(r,\omega)$ are recorded. French (1975) and Schneider (1978) showed that if the data are collected in a flat plane, the second term in the integrand of the Kirchhoff equation is the negative of the first term. This condition is approximately valid for borehole profiling, since any change of borehole direction must proceed gradually and may be assumed negligible for typical seismic wavelengths. We therefore replace the second term containing the normal derivative of the data with the negative of the first term. Also, we extend the boundary ofthe integration surface to infinite distance, where there is no back-scattered energy as governed by the radiation conditions, so the only remaining contribution to the integral comes from the recording surface S. Equation (4) becomes

$$P(r,\omega) = 2\int_S P(r_g,\omega)\partial_n G dS \qquad (5)$$

We now write $G = A(r|r_g)e^{-i\omega\tau(r|r_g)}$ and use the geometrical optics approximation for the amplitude $A(r|r_g)$ and phase $\tau(r|r_g)$. The negative sign in the phase of G is taken because we shall be extrapolating backward in time. Along a ray path, the variation in $e^{-i\omega\tau}$ is much larger than the variation in A. Thus the first term in the derivative of G

$$\partial_n G = (\partial_n A)e^{-i\omega\tau} - Ae^{-i\omega\tau} i\omega(\partial_n \tau) \qquad (6)$$

is small compared to the second term and is neglected. The Kirchhoff integral (5) can now be written in the form

$$P(r,\omega) = -2\int_S P(r_g,\omega) A\, e^{-i\omega\tau} i\omega(\partial_n \tau) dS \qquad (7)$$

in which

$$\partial_n \tau = n \cdot \partial\tau = n \cdot t / v_g = \cos\theta_g / v_g \qquad (8)$$

where t is the unit tangent vector for the emerging ray, and θ_g is the angle of emergence, and v_g is the acoustic velocity at the receiver. The amplitude term $A(r|r_g)$ can be obtained from the transport equation.

The reflectivity function $R(r,\omega)$ is defined as the ratio of the back-propagated field from the receivers $P(r,\omega)$ to the incidence field from the source $P_s(r,\omega)$ (Claerbout, 1970),

$$R(r,\omega)=\frac{P(r,\omega)}{P_s(r,\omega)} \qquad (9)$$

The incidence source field is approximated by the WKBJ Green's function

$$P_s(r,\omega)=A(r|r_s)e^{i\omega\tau(r|r_s)} \qquad (10)$$

Combining equations (7) and (9) gives the holographic (i.e., frequency-domain) form of Kirchhoff migration. The time-space domain reflectivity is obtained by an inverse Fourier transform,

$$R(r)=-2\int_S \frac{A(r|r_g)}{A(r|r_s)}\frac{\cos\theta_g}{v_g}\partial_t P(r_g,\tau(r|r_s)+\tau(r|r_s))dS \qquad (11)$$

TRANSMISSION MULTIPLE REFLECTIONS AND CHANNEL WAVES

In this study, I use an earth section model 600 ft in depth and 184 ft in horizontal separation, Figure 1. The medium has a constant reference acoustic velocity of 18000 ft/s. At the depth of 300 ft and 400 ft, there are two thin low velocity layers of acoustic velocity 10000 ft/s, the thickness is 2.5 ft or two grid points in discrete representation.

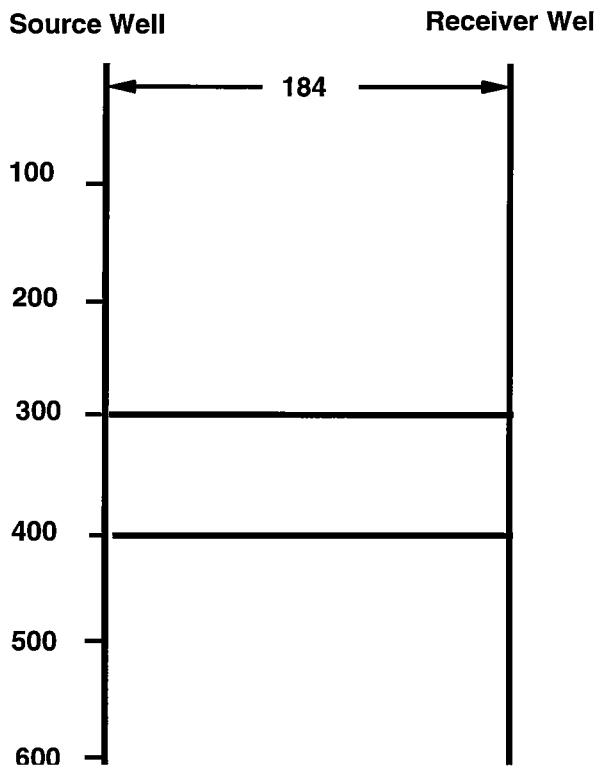

Figure 1: Cross well earth model

Figure 2 shows two finite-difference modeling common shot gather data. In the first gather, the source is above the two reflectors at 140 ft. The data shows distinct direct arrival, primary upgoing reflections from the two reflectors, transmission multiple and much weaker upgoing multiple. The upgoing multiple undergoes one more reflection than the transmission multiple, so that its amplitude is an order of magnitude weaker. In this modeling the record length of 50 ms is the record length of an actual field survey. As a result, higher order multiples are not recorded. Thus, we focus our analysis at the transmission multiples.

In the second gather, the source is located in the low velocity layer at 300 ft, so that channel waves are generated. The reflection event of the upper reflector coalesces into the direct arrival.

Figure 3 shows the pre-stack Kirchhoff migration images of the previous two common shot gather data. According to the analysis of multiples in (Mo, 1995), the equivalence of transmission multiples and primary reflections.

$$H = S - n(H_2 - H_1) \qquad (12)$$

where S is the source depth, H_2 and H_1 are the depths of two reflectors, n is the order of transmission multiples, and then H is the depth of the equivalent primary reflection.

In Figure 3 (a) the source at 140 ft, the speudo-primary reflection image event of the first order transmission multiple appears at the depth of 40 ft. In Figure 3 (b) the source at 300 ft, the speudo-primary reflection image event of the first order transmission multiple appears at the depth of 200 ft. The imaging events of the channel waves appear as horizontal ellipses.

Figure 4 shows some common radiation angle images. The image events of the transmission multiples appear as the vertical events. And the image events of the channel waves align along the radiation directions.

Figures 5, 6, and 7 show common shot gather data, pre-stack migration images, and common radiation angle images for a complicated reflector model.

RANDOM NOISES

Random noise data are modeled by

$$n(t) = f(t) * w(t) \qquad (13)$$

where $f(t)$ is modeled as Gaussian distribition random signal, the mean of which is zero and the standard variation equals to the amplitude of the reflection signal, and $w(t)$ is the same as the source wavelet function.

Figure 8 shows a common shot gather data with Gaussian random noises. The signal/noise ratio is 1 in the data. Figure 9 shows the corresponding pre-stack Kirchhoff migration image, the signal/noise ratio increases greatly as compared to the data. It is convincing by comparing this image of noisy input data with the image Figure 6 of input data without noises. The pre-stack migration is performed by applying the Kirchhoff migration integral equation (11). Figure 10 shows some common radiation angle images.

CONCLUSIONS

Imaging effects of transmission multiples are equivalent to primary reflectins. And their imaging speudo-depths have linear relationship with the source depth. As a result, after radiation angle transformation on the prestack image volume the image events of the transmission multiples appear vertically in common radiation angle images.

Channel waves in cross-well seismic survey appear in the receiver traces horizontally across the source. Imaging effects of channel waves in pre-stack migration appear as ellipses with the locations of the source and the hirozontal receiver as the foci. As a result, the image events of the channel waves align along the radiation angle direction in common radiation angle images.

By definition, in pre-stack migration operation signals are summed constructively and random noises are summed distructively. Pre-stack migration increases signal/noise ratio. Signal/noise ratio is higher in pre-stack migration images than in common shot gather data.

REFERENCES

Goodman, J., 1970,
Introduction to Fourier Optics.

Mo, L., and Harris, J. M., 1995,
Travel time equations in cross-well seismic profiling: STP-5.

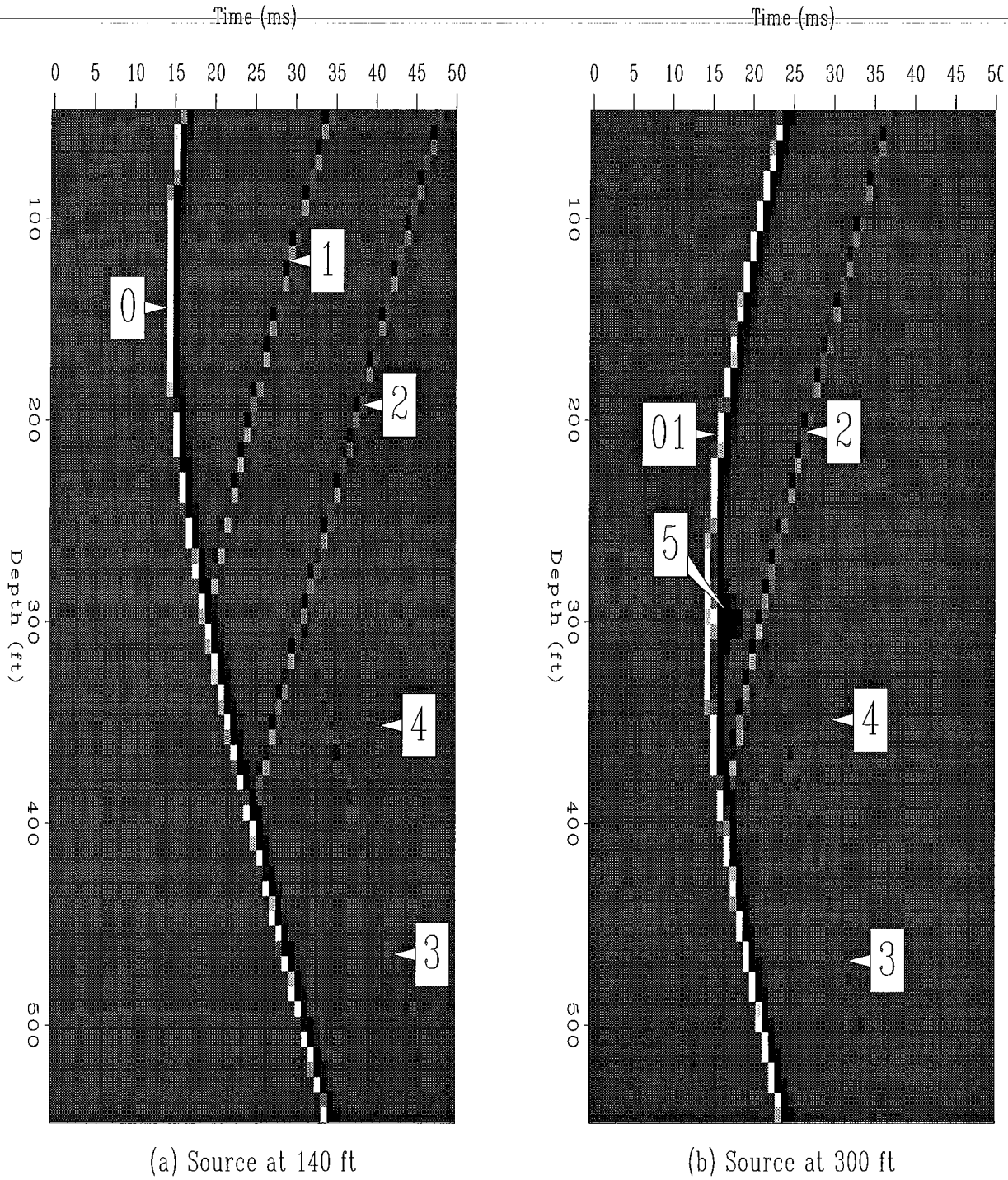

(a) Source at 140 ft (b) Source at 300 ft

Figure 2: Common shot gather data in model with two reflectors. 0 is the direct arrival, 1 primary reflection from the upper reflector, 2 primary reflection from the lower reflector, 3 transmission multiple, 4 upgoing multiple, and 5 channnel wave.

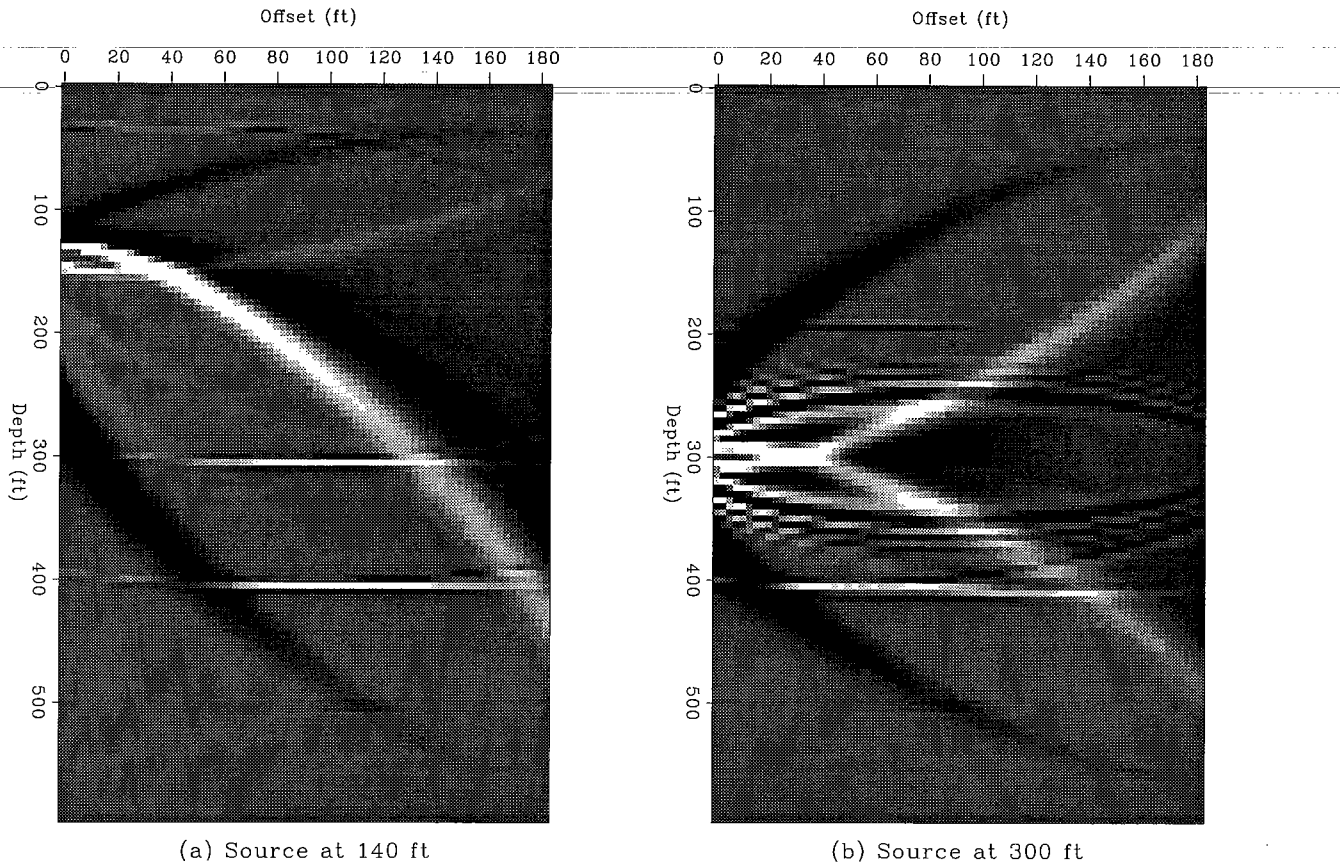

Figure 3 : Prestack migration images.

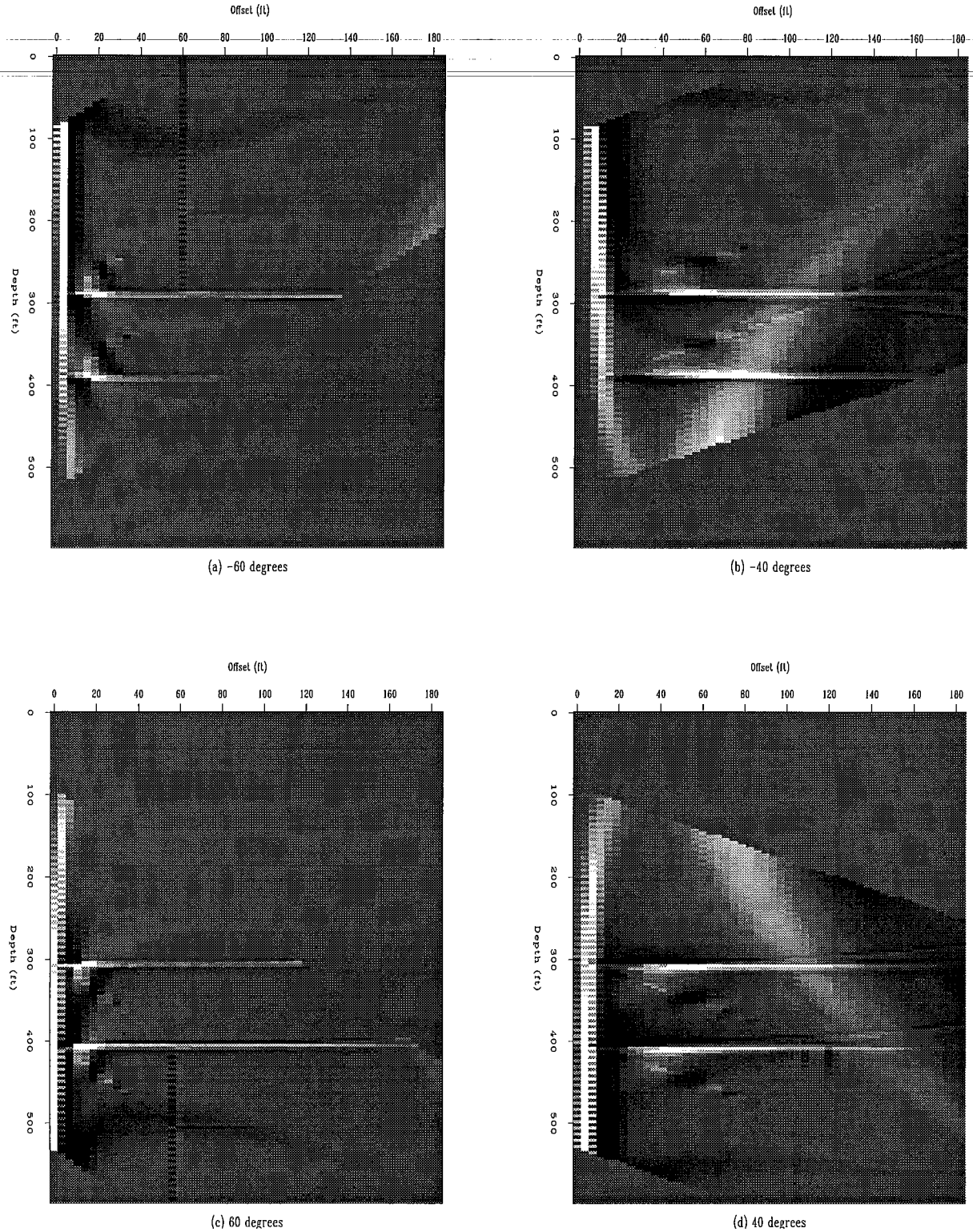

Figure 4: Common radiation angle images.

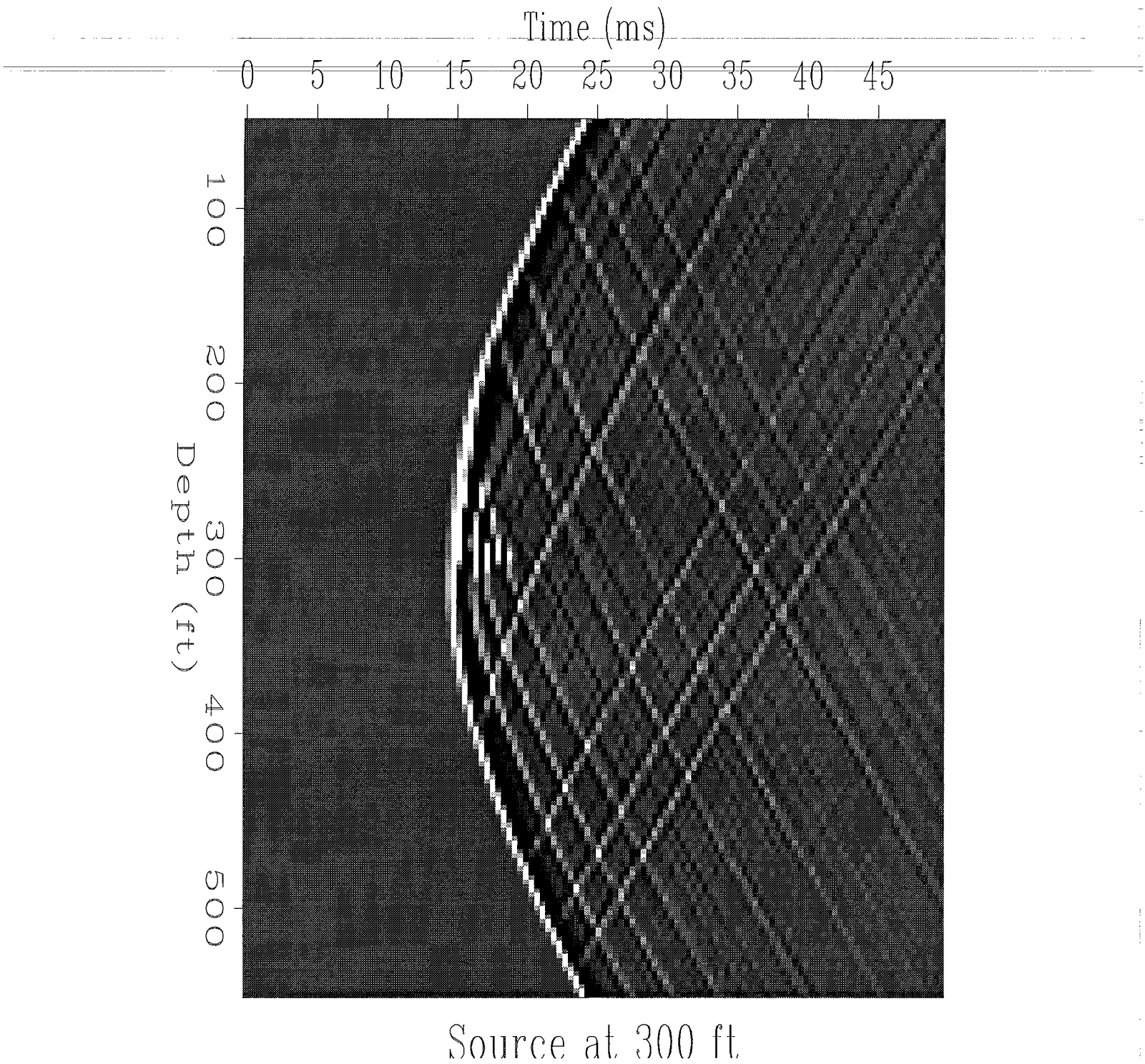

Figure 5: Common shot gather data.

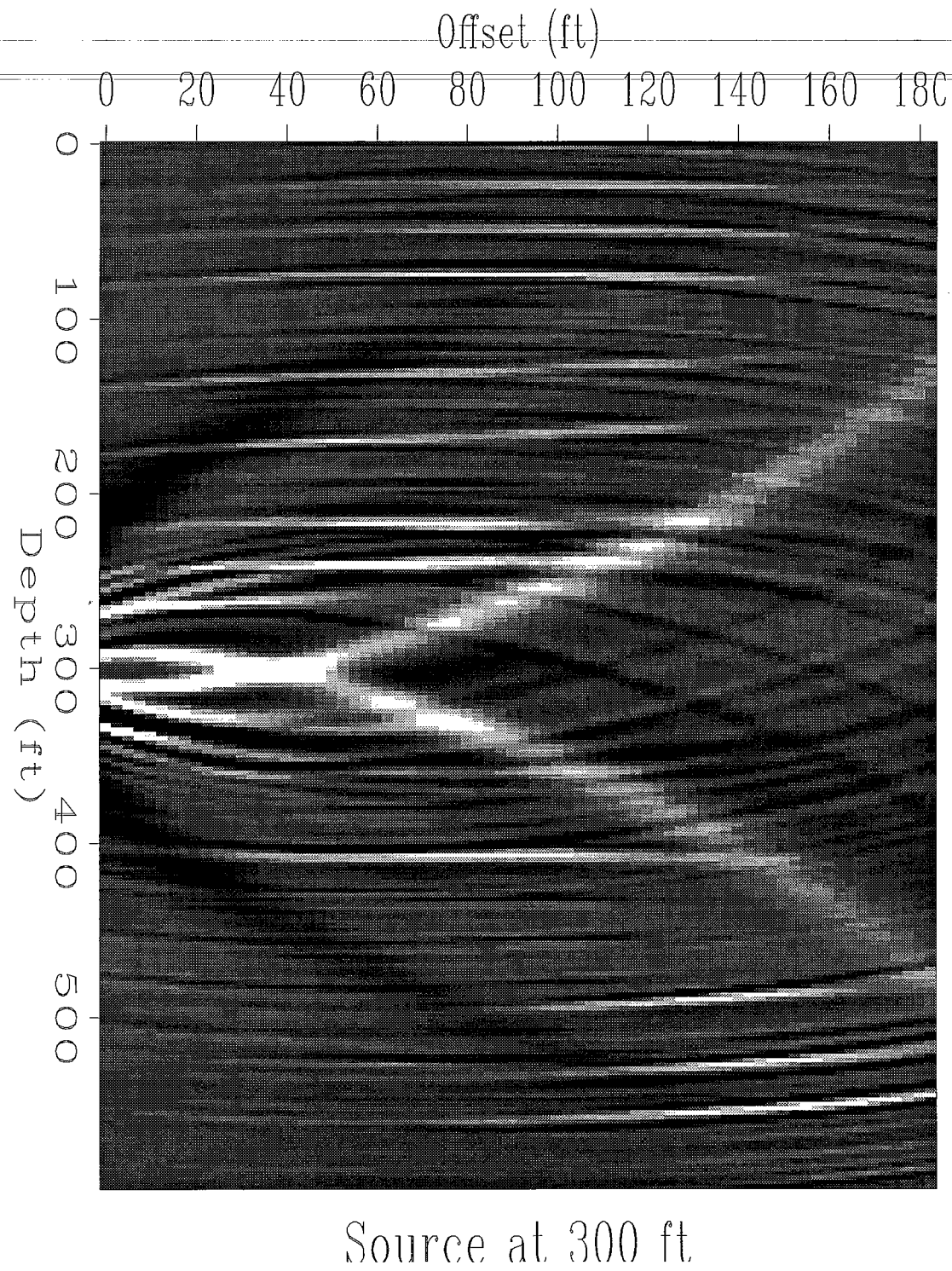

Figure 6: Prestack migration image.

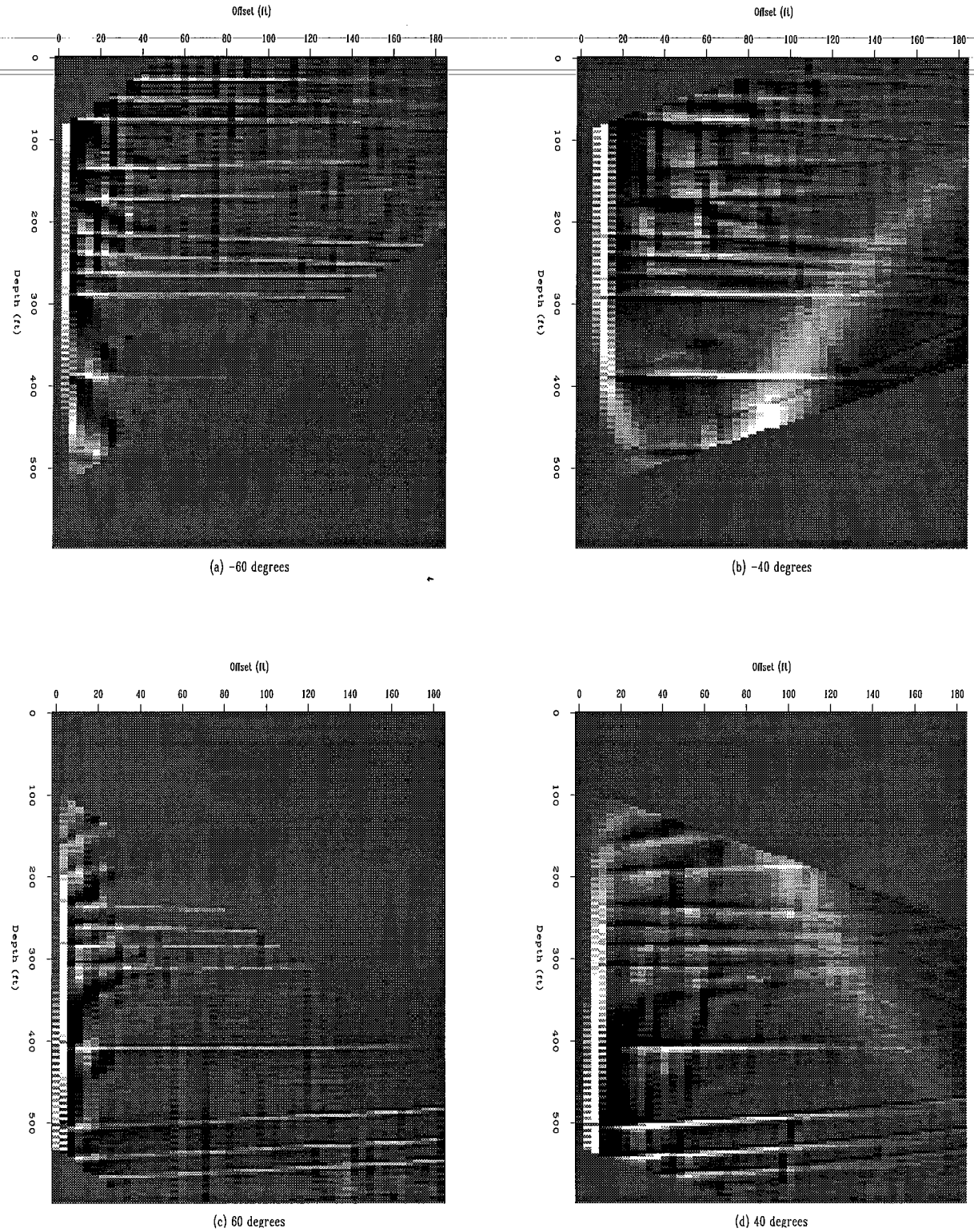

Figure 7: Common radiation angle images.

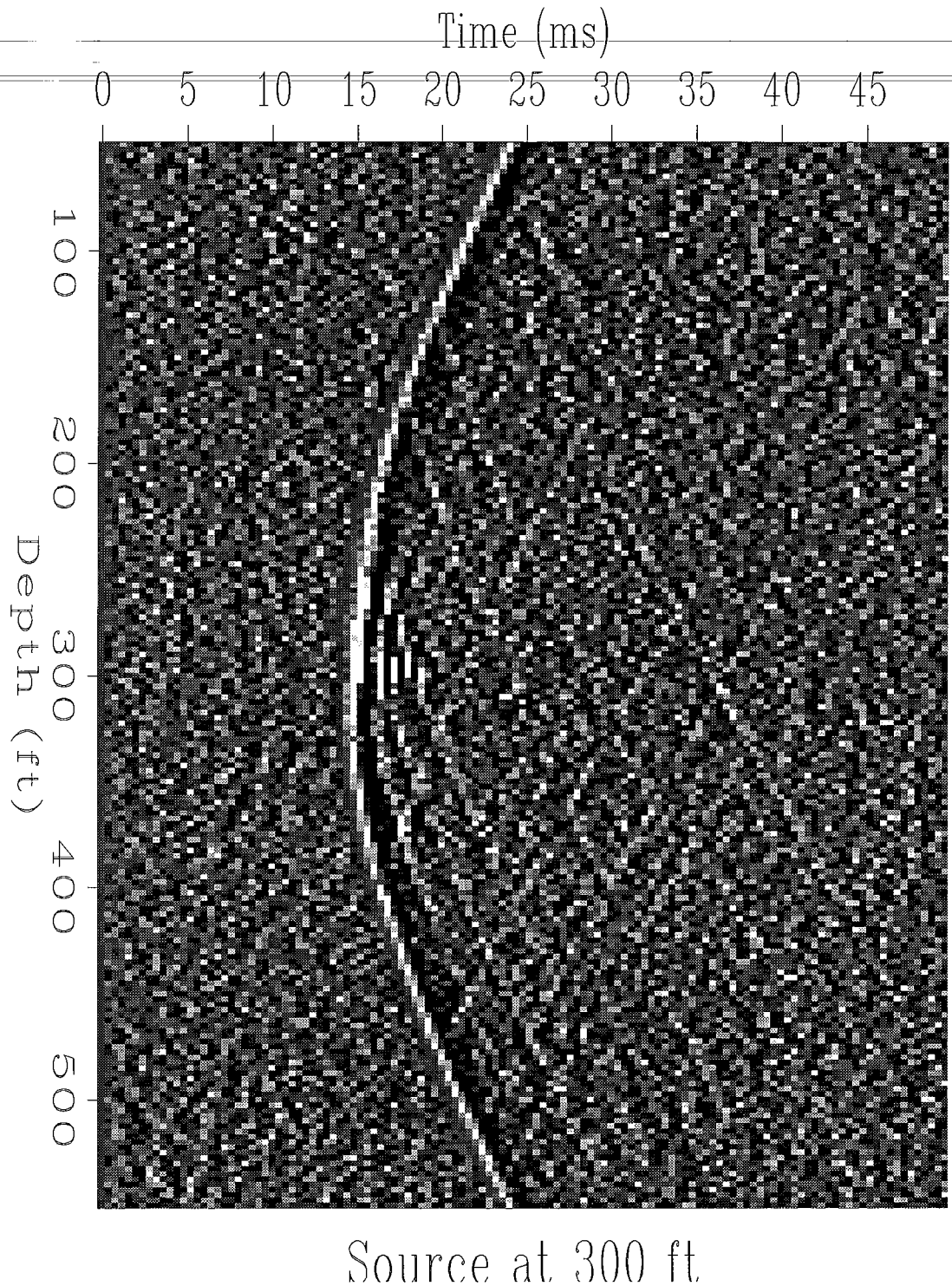

Figure 8: Common shot gather data.

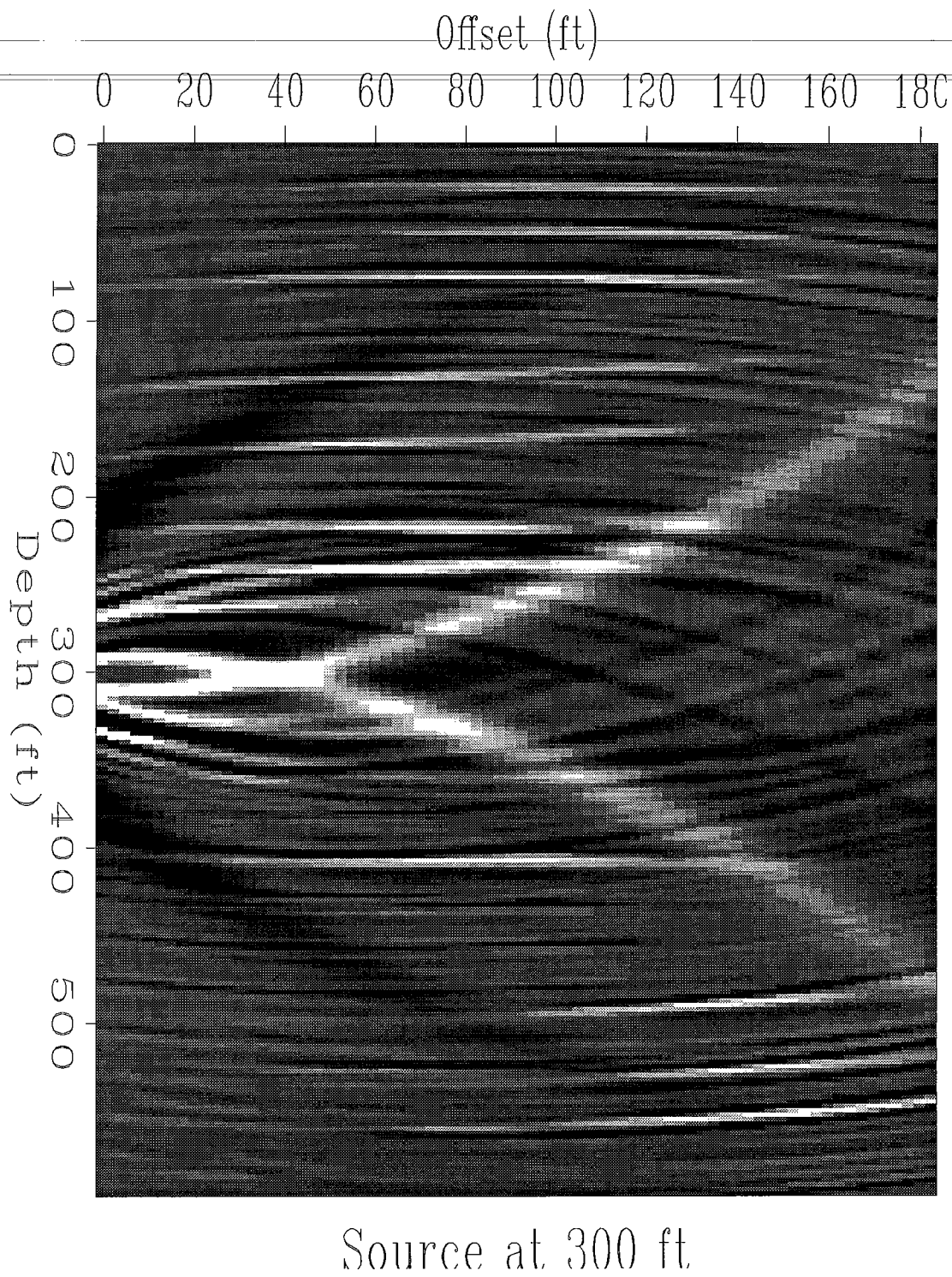

Figure 9: Prestack migration image.

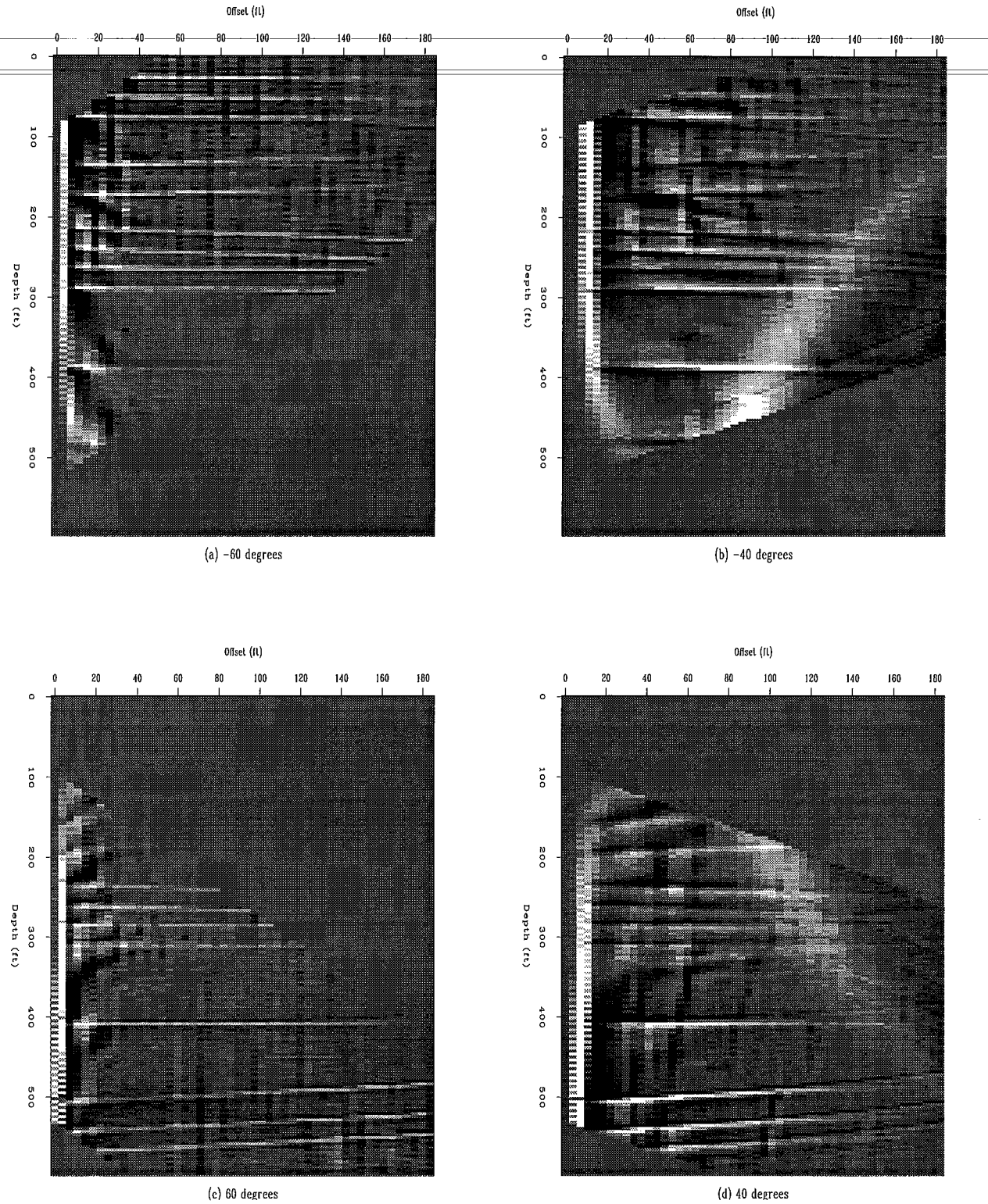

(a) -60 degrees

(b) -40 degrees

(c) 60 degrees

(d) 40 degrees

Figure 10: Common radiation angle images.